Published OnlineFirst February 10, 2015; DOI: 10.1158/0008-5472.CAN-14-1924

Tumor and Stem Cell Biology

Cancer Research

Aldehyde Dehydrogenase Is Regulated by β-Catenin/TCF and Promotes Radioresistance in Prostate Cancer Progenitor Cells

Monica Cojoc[1], Claudia Peitzsch[1], Ina Kurth[1], Franziska Trautmann[1], Leoni A. Kunz-Schughart[1], Gennady D. Telegeev[2], Eduard A. Stakhovsky[3], John R. Walker[4], Karl Simin[5], Stephen Lyle[5], Susanne Fuessel[6], Kati Erdmann[6], Manfred P. Wirth[6], Mechthild Krause[1,7,8,9], Michael Baumann[1,7,8,9], and Anna Dubrovska[1,9]

Abstract

Radiotherapy is a curative treatment option in prostate cancer. Nevertheless, patients with high-risk prostate cancer are prone to relapse. Identification of the predictive biomarkers and molecular mechanisms of radioresistance bears promise to improve cancer therapies. In this study, we show that aldehyde dehydrogenase (ALDH) activity is indicative of radioresistant prostate progenitor cells with an enhanced DNA repair capacity and activation of epithelial–mesenchymal transition (EMT). Gene expression profiling of prostate cancer cells, their radioresistant derivatives, $ALDH^+$ and $ALDH^-$ cell populations revealed the mechanisms, which link tumor progenitors to radioresistance, including activation of the WNT/β-catenin signaling pathway. We found that expression of the *ALDH1A1* gene is regulated by the WNT signaling pathway and co-occurs with expression of β-catenin in prostate tumor specimens. Inhibition of the WNT pathway led to a decrease in $ALDH^+$ tumor progenitor population and to radiosensitization of cancer cells. Taken together, our results indicate that $ALDH^+$ cells contribute to tumor radioresistance and their molecular targeting may enhance the effectiveness of radiotherapy. *Cancer Res; 75(7); 1482–94. ©2015 AACR.*

Introduction

Prostate cancer is the most commonly diagnosed noncutaneous neoplasm in men worldwide (1). Most of the patients with prostate cancer are diagnosed at an early stage and may be cured with surgery or radiotherapy, with or without androgen deprivation (1–3). Depending on tumor stage, from 55% to more than 90% of all prostate cancers can be permanently controlled by radiotherapy (3–5). This supports that radiotherapy has significant potential to inactivate tumor-initiating or cancer stem cells (CSC), which can potentially provoke tumor relapse. Nevertheless, some patients with high-risk prostate cancer develop local relapse after radiation therapy. The most obvious explanation for radiotherapy failure is related to the CSC population, which was not completely sterilized during the treatment and caused tumor recurrence (6, 7).

The proportion of CSCs in the bulk tumor cell population has a high intertumoral variability. Few studies have correlated the density of CSC markers with poor clinical outcome of patients with head and neck squamous cell carcinomas (HNSCC), glioma, cervical squamous cell carcinoma, and rectal carcinoma (7, 8). Despite the expression of CSC markers varies considerably between tumors of the same entity, the current findings suggest that estimation of the number of CSCs in pretherapeutic biopsies is of high importance for prediction of tumor radiocurability and selection of the optimal therapy (6). However, the clinical and preclinical studies analyzing the predictive value of CSC biomarkers on prostate cancer radiocurability are missing so far.

Aside from the impact of CSC density on tumor radiocurability, recent experimental reports suggest a number of different intrinsic and extrinsic adaptations that confer tumor radioresistance and that also occur in CSC populations, including senescence, increased DNA repair capability, intracellular scavenging of reactive oxygen species (ROS), and activation of cell survival pathways (8). All these mechanisms are dynamic in nature due to the plasticity of CSC

[1]OncoRay-National Center for Radiation Research in Oncology, Medical Faculty and University Hospital Carl Gustav Carus, Technische Universität Dresden and Helmholtz-Zentrum Dresden-Rossendorf, Fetscherstrasse, Dresden, Germany. [2]Institute of Molecular Biology and Genetics NAS of Ukraine, Kyiv, Ukraine. [3]National Cancer Institute, Kyiv, Ukraine. [4]Genomics Institute of the Novartis Research Foundation, San Diego, California. [5]UMass Cancer Center Tissue Bank, Department of Cancer Biology, UMass Medical School, Worcester, Massachusetts. [6]Department of Urology, Medical Faculty and University Hospital Carl Gustav Carus, Technische Universität Dresden, Fetscherstrasse, Dresden, Germany. [7]Department of Radiation Oncology, Medical Faculty and University Hospital Carl Gustav Carus, Technische Universität Dresden, Fetscherstrasse, Dresden, Germany. [8]Institute of Radiation Oncology, Helmholtz-Zentrum Dresden-Rossendorf, Germany, Bautzner Landstrasse, Dresden, Germany. [9]German Cancer Consortium (DKTK) Dresden and German Cancer Research Center (DKFZ), Heidelberg, Germany.

Note: Supplementary data for this article are available at Cancer Research Online (http://cancerres.aacrjournals.org/).

M. Cojoc and C. Peitzsch contributed equally to this article.

Corresponding Authors: Anna Dubrovska, OncoRay-National Center for Radiation Research in Oncology, Medical Faculty and University Hospital Carl Gustav Carus, Technische Universität Dresden, Fetscherstr.74/PF41 01307 Dresden, Germany. Phone: 49-351-458-7150; Fax: 49-0351-458-7311; E-mails: Anna.Dubrovska@OncoRay.de; and Claudia Peitzsch, Claudia.Peitzsch@OncoRay.de

doi: 10.1158/0008-5472.CAN-14-1924

populations and multiplicity of the microenvironmental conditions that can differently contribute to the CSC response to irradiation through the course of therapy (8, 9).

Identification of predictive biomarkers for individualized radiotherapy and characterization of the molecular mechanisms by which prostate tumor–initiating cells can survive treatment may ultimately lead to more efficient cancer treatment. In this study, we show that aldehyde dehydrogenase (ALDH) activity is indicative of prostate tumor progenitors with increased radioresistance, improved DNA double-strand break repair, and activation of signaling pathways, which promote epithelial–mesenchymal transition (EMT) and migration.

Radioresistant (RR) derivatives of established prostate cancer cell lines share many properties with tumor progenitor cells, including an enhanced expression of CSC markers (CD133, CXCR4, ABCG2, OCT4, NANOG), high ALDH activity, induction of EMT, and an increase in DNA repair capacity. mRNA expression analysis of the prostate cancer cells, their radioresistant derivatives, and $ALDH^+$ tumor progenitor population revealed common signaling pathways, which link CSCs to radioresistant cancer cells and include WNT/β-catenin, G-protein–coupled receptor, TGFβ, and integrin signaling pathways. This is, to our knowledge, the first study showing that expression of the *ALDH1A1* gene is directly regulated by β-catenin/TCF transcriptional complex. Consistent with these results, inhibition of the WNT/β-catenin signaling pathway by the tankyrase inhibitor XAV939 or siRNA-mediated knockdown of β-catenin expression led to a decrease in the $ALDH^+$ cell population and radiosensitization of prostate cancer cells.

Taken together, our data suggest that $ALDH^+$ cell population contributes to prostate tumor radioresistance and that targeting this cell population may be beneficial in prostate cancer treatment.

Materials and Methods

Cell lines and culture condition

Prostate cancer cell lines DU145, PC3, and LNCaP were purchased from ATCC and cultured according to the manufacturer's recommendations in a humidified 37°C incubator supplemented with 5% CO_2. DU145 and PC3 cell lines were maintained in DMEM (Sigma-Aldrich) and LNCaP cells in RPMI-1640 (Sigma-Aldrich), both supplemented with 10% FBS (PAA Laboratories) and 2 mM L-glutamine (Sigma-Aldrich). All cell lines were genotyped using microsatellite polymorphism analysis and tested for mycoplasma directly before experimentation.

Human tissue samples and preparation of cell suspension

Clinical material was collected at Massachusetts tissue bank, Department of Urology of Medical Faculty at Technical University Dresden (Dresden, Germany), and Kyiv National Cancer Institute (Kyiv, Ukraine) with informed consent and approval from the local ethics committees (Office of the Vice Provost for Research, Human Subjects Research 55 Lake Ave North Worcester, Massachusetts 01655, FWA #00004009, docket #H-11731; Institutional review board of the Medical Faculty at the Technical University of Dresden, EK195092004 and EK194092004; Ethics Committee of Kyiv National Cancer Institute, 33-34, Lomonosova str, 02166 Kyiv, Ukraine, protocol no. 44). Primary tumor tissues used in the study are described in Supplementary Table S1.

Animals and *in vivo* tumorigenicity assay

The animal facilities and the experiments were approved according to the institutional guidelines and the German animal welfare regulations (protocol number 24-9168.11-1/2010-21). The experiments were performed using 8- to 12-week-old male NMRI (*nu*/*nu*) mice obtained from the animal breeding facility (Experimental Centre, Medical Faculty, Technical University Dresden). To immunosuppress the nude mice further, the animals underwent total body irradiation 1 to 3 days before tumor transplantation with 4 Gy (200 kV X-rays, 0.5 mm Cu filter, 1 Gy/min). Mice were examined once a week and relative tumor volume (mm^3) based on caliper measurements was calculated as (length × width × height)/2. At tumor volume of 100 mm^3, mice were counted as tumor bearing to calculate tumor uptake and Kaplan–Meier plots were analyzed using the log-rank test (GraphPad Prism 5). The mice were observed for 100 days for tumor appearance and development. Xenograft tumors were excised, fixed in 4% paraformaldehyde overnight, and kept in 30% sucrose before embedding in TissueTek O.C.T compound (Sakura Finetek). Tissue sectioning was performed using Microm HM 560, Cryo-Star cryostat. Xenograft tumors were histopathologically and immunohistochemically examined by a pathologist following diagnostic protocols of the Department of Pathology, University Hospital Dresden. For flow cytometric analysis, the single-cell suspension was obtained after 1-hour incubation at 37°C in DMEM containing collagenase Type 3 (Worthington) and mechanical dissociation using the Gentle MACS Dissociator (Miltenyi Biotec). Samples for Western blot analysis were flash-frozen in liquid nitrogen. Analysis of the tumor-initiating cell frequency was performed using the web-based ELDA (extreme limiting dilution analysis) statistical software, which uses the frequency of tumor-positive and -negative animals at each transplant dose to determine the frequency of tumor-initiating cells within the injected cell populations (9).

Microarray analysis of the prostate cancer cell lines

Gene expression profiling of the DU145, DU145-RR, $ALDH^+$ DU145, $ALDH^-$ DU145, $ALDH^+$ DU145-RR, $ALDH^-$ DU145-RR cells was performed using SurePrint G3 Human Gene Expression 8 × 60 K v2 Microarray Kit (Design ID 039494, Agilent Technologies) according to the manufacturer's recommendations. Total RNA was isolated from cell pellets using the RNeasy Kit (Qiagen). Sample preparation for analysis was carried out according to the protocol detailed by Agilent Technologies. Briefly, first and second cDNA strands were synthesized; double-stranded cDNA was *in vitro* transcribed using the Low Input Quick Amp Labeling Kit; and the resulting cRNA was purified and hybridized to oligonucleotide arrays (SurePrint G3 Human Gene Expression 8 × 60 K v2 Microarray, Design ID 039494) representing about 60,000 features, including 27,958 Entrez Gene RNAs and 7,419 lincRNAs. Arrays were processed using standard Agilent protocols. Probe values from image files were obtained using Agilent Feature Extraction Software. The dataset was normalized using GeneSpring software, and the list of differentially regulated genes with fold change >2 and $P < 0.05$ was further analyzed using a web-based Panther Pathway Analysis tool. Data deposition: all data are MIAME compliant and raw data have been deposited in the Gene Expression Omnibus (GEO) database, accession no GSE53902.

Published OnlineFirst February 10, 2015; DOI: 10.1158/0008-5472.CAN-14-1924

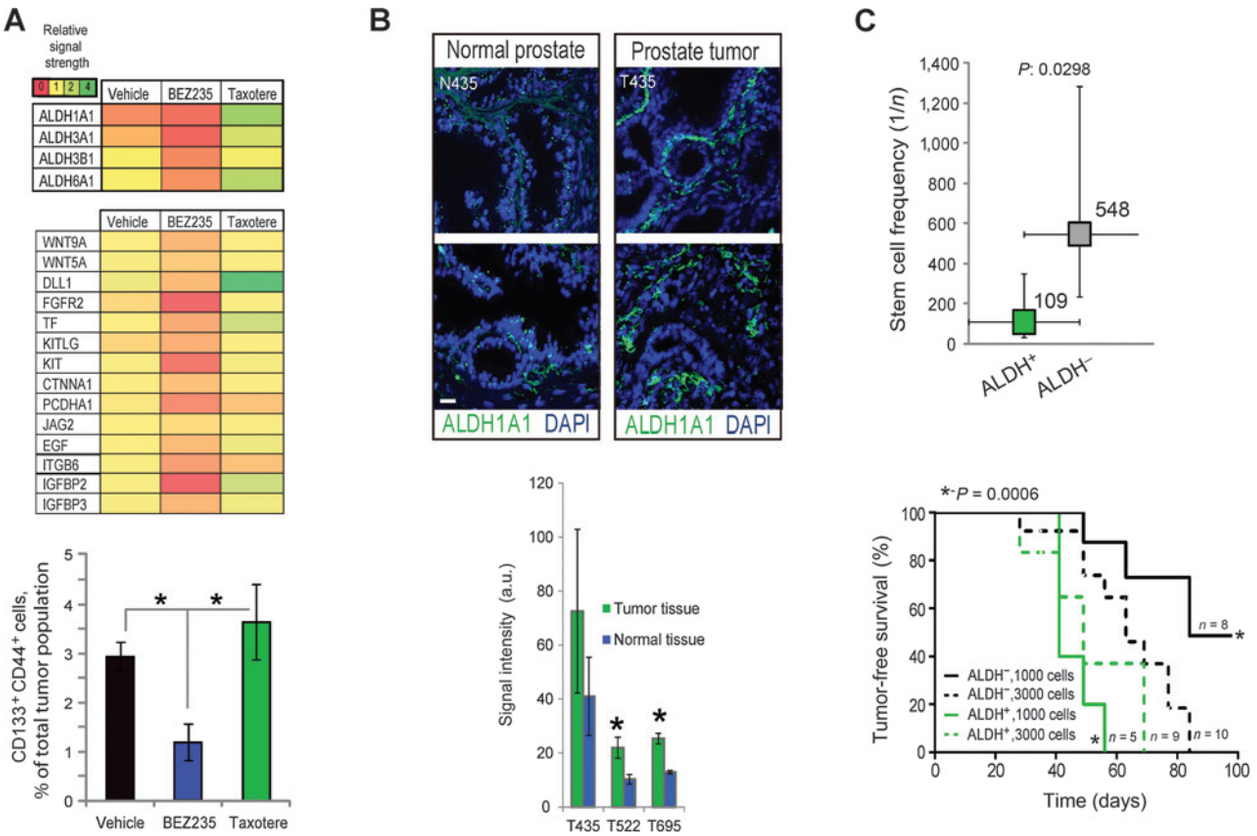

Figure 1.
Expression of ALDH genes correlates with survival of cancer progenitors in xenograft tumors and is upregulated in prostate carcinoma tissues. A, analysis of $CD133^+/CD44^+$ cancer progenitor population and gene expression in xenograft tumors treated with PI3K inhibitor NVP-BEZ235. Error bars, SD. *, $P < 0.05$. B, representative images of IHC analysis showing an expression of ALDH1A1 in prostate tumors and normal adjacent tissues. Three formalin-fixed, paraffin-embedded prostate tumor specimens were analyzed. Scale bar, 50 μm. Error bars, SEM., $P < 0.05$. C, $ALDH^+$ cells possess higher tumorigenic properties compared with $ALDH^-$ cells. Limiting dilution assay calculations were performed using the ELDA software.

Statistical analysis

The results of colony formation assays, microscopy image analysis, Transwell migration assay, luciferase reporter assay, flow cytometric analysis, cell proliferation assays, and *in vivo* tumorigenicity assays were analyzed by a paired *t* test. $P < 0.05$ was regarded as statistically significant.

Results

Prostate cancer cells with a high ALDH activity have stem cell–like properties

Previous studies have shown the existence of cancer progenitor populations in prostate tumors and established cell lines. These progenitor cells have been characterized by the expression of the surface markers CD44, CD133, integrin α2β1, and high ALDH activity (10–13). The inhibition of PI3K activity by the chemical inhibitor NVP-BEZ235 led to a significant decrease in the population of prostate tumor–initiating cells in DU145 prostate xenograft tumors. In contrast, the use of the cytotoxic drug Taxotere resulted in a decrease in proliferating tumor cells but led to an overall increase in the population of cancer progenitor cells *in vivo* (12). To identify genes, for which expression levels correlate with the dynamics of $CD44^+/CD133^+$ progenitor cell population in DU145 xenograft tumors, we performed a whole-genome gene expression profiling of the xenograft tumors from mice that received Taxotere (10 mg/kg, intravenously) once per week for 4 weeks, the dual PI3K/mTOR inhibitor NVP-BEZ235 (12.5 mg/kg, orally) once per day for 4 weeks, or were treated with vehicle, as described earlier (Fig. 1A; ref. 12).

Comparative analysis of gene expression profiles has shown that transcription of the different ALDH isoforms, including *ALDH1A1*, *ALDH3A1*, *ALDH3B1*, and *ALDH6A1*, correlates with the percentage of $CD44^+/CD133^+$ cancer progenitors in xenograft tumors as well as with expression of other stem cell and developmental genes, including *WNT5A*, *WNT9A*, *DLL1*, *FGFR2*, *KIT*, *KITLG*, *CTNNA1*, *EGF*, *IGFBP2*, and *IGFBP3* (Fig. 1A).

Analysis of the Oncomine database and immunostaining of tumor specimens revealed that expression of the ALDH isoforms, such as *ALDH1A1* and *ALDH6A1*, was significantly increased in primary prostate carcinoma tissues as compared with the normal prostate gland (Fig. 1B; Supplementary Fig. S1A). Strikingly, a gene signature, which includes expression of *ALDH1A1*, *ALDH3B1*, *ALDH6A1 CD44*, and *PROM1* (CD133) correlated with reduced disease-free survival in patients with prostate cancer. Data are based on the Taylor study (Supplementary Fig. S1B; ref. 14).

To analyze whether the cells with a high ALDH activity isolated from prostate cancer cell lines have functional characteristics of tumor progenitor cells, we examined their clonogenic,

Published OnlineFirst February 10, 2015; DOI: 10.1158/0008-5472.CAN-14-1924

spherogenic, and tumorigenic properties. Prostate cancer cells that have a high level of ALDH activity can be enriched from prostate cancer cell lines by growing them under serum-free prostatosphere-forming conditions (Supplementary Fig. S2A). We and others have shown that prostate cell populations expanded under these conditions have increased clonogenic potential *in vitro* and tumorigenic potential *in vivo* (13, 15). $ALDH^+$ cell populations isolated by FACS from DU145 and PC3 cells showed an increase in their colony- and sphere-forming abilities over $ALDH^-$ cells (Supplementary Fig. S2B–S2D). To determine the frequency of tumor-initiating cells within $ALDH^+$ and $ALDH^-$ prostate cancer cell populations, we used an *in vivo* limiting dilution analysis. The highly purified $ALDH^+$ and $ALDH^-$ DU145 cells at varying cell numbers (100, 1,000, and 3,000 cells) were injected subcutaneously into athymic immunodeficient NMRI *nu/nu* mice. Animals alive and tumor-free at the end of the observation period (100 days) were defined as long-term survivors. The $ALDH^+$ population showed a significantly higher tumor uptake rate and a higher frequency of tumor-initiating cells than $ALDH^-$ cell population [1/109 (at 95% confidence interval, CI, 1/349 to 1/35 cells) and 1/548 (at 95% CI: 1/1285 to 1/234 cells), respectively; $P < 0.03$; Fig. 1C].

Next, we analyzed whether $ALDH^+$ and $ALDH^-$ cells are capable of recapitulating the populations of the original cell lines. The DU145 cell line consisted of 8.3% of $ALDH^+$ cells and 91.7% of $ALDH^-$ cells was sorted into $ALDH^+$ and $ALDH^-$ populations, which were maintained in standard tissue culture conditions. The cells were cultured for a period of 14 days and then analyzed by flow cytometry. We found that prolonged culture resulted in the reversion of both populations to a bimodal profile. The $ALDH^+$ population gave rise to the cell population, which included 22.2% $ALDH^+$ cells and 77.8% $ALDH^-$ cells. These cell frequencies are closer to the cell population ratio in the original unsorted cell population compared with the cell population generated by $ALDH^-$ cells (1.8% $ALDH^+$ cells and 98.2% $ALDH^-$ cells). Similar results were obtained when the same experiment was performed with PC3 cells (Supplementary Fig. S2E). Cell viability assay revealed no statistical difference between growth and viability of $ALDH^+$ and $ALDH^-$ cells (Supplementary Fig. S2F). To determine whether $ALDH^+$ and $ALDH^-$ cells exhibit distinct differentiation potential *in vivo*, we analyzed the expression of prostate lineage markers in xenograft tumors derived from FACS-purified $ALDH^+$ or $ALDH^-$ cells. The xenograft tumors originated from both $ALDH^+$ and $ALDH^-$ cell subsets included a $CK5^+$ population of basal epithelial cells and $CK18^+$ population of luminal epithelial cells. However, $ALDH^-$ cells were less efficient to generate $CK5^+$ cell population *in vivo* as compared with $ALDH^+$ cells (Supplementary Fig. S2G).

Dynamics of the stem cell markers in prostate cancer cells in response to irradiation

Recent findings suggest that X-ray irradiation leads to enrichment of the CSC population (16, 17). To analyze the radiation-induced changes in the number of progenitor cells, we treated established prostate cancer cell lines and primary prostate tumor cells with fractions of 2 or 4 Gy of X-ray irradiation and assessed the expression of CSC markers by flow cytometry, Western blotting, and immunohistochemistry (IHC) 7 days after irradiation. We have found that irradiation led to a dose-dependent increase in the fraction of DU145 and LNCaP cells with a high ALDH activity, a high expression of CSC markers, such as CD133, CXCR4, ABCG2, as well as to upregulation of AKT phosphorylation at Ser 473 and increase of expression of the transcription regulators NANOG and β-catenin (Fig. 2A–C; Supplementary Fig. S3A). We found that $CD133^+/CD44^+$ cell population was increased in 22Rv1 prostate cancer cells about 20-fold after fractionated irradiation with 7×2 Gy of X-ray. In contrast to the prostate cancer cells, population of $CD133^+/CD44^+$ cells was decreased in normal prostate epithelial cells RWPE-1 upon irradiation (Supplementary Fig. S3B).

Furthermore, we assessed the enrichment of tumor progenitors in primary prostate tumor specimens. In this study, we used single-cell suspensions obtained from three freshly isolated human prostate cancer specimens. The cells were plated and irradiated with 2 Gy of X-ray the following day and 3 days later. Four days after irradiation, we assessed the number of $ALDH1A1^+$, $ALDH1A3^+$, and $ALDH1A1^+/ALDH1A3^+$ cells by fluorescence microscopy and found that irradiation led to significant enrichment of these cell populations in the tumor specimens (Fig. 2D and E; Supplementary Fig. S3C).

$ALDH^+$ prostate progenitor cells are radioresistant

Several findings suggest that CSCs might be less sensitive to irradiation than non-CSCs in *in vitro* assays (8). However, these reports still remain controversial (9). We used clonogenic and spherogenic radiobiological cell survival assays to analyze the relative radioresistance of $ALDH^+$ and $ALDH^-$ cell populations. FACS-purified $ALDH^+$ and $ALDH^-$ cells were plated as single-cell suspension, irradiated with a single dose of 2, 4, or 6 Gy of X-ray, and cultured under colony- and sphere-forming conditions. Both clonogenic and spherogenic survival assays demonstrated a significantly higher radioresistance of $ALDH^+$ cells in DU145 and PC3 cell lines than $ALDH^-$ cells (Fig. 3A and B). Remarkably, not only the number but also the size of the colonies formed by $ALDH^+$ cells after X-ray treatment was increased as compared with the colonies derived from $ALDH^-$ cells, showing both a higher survival rate and a higher proliferative capacity of $ALDH^+$ cells after irradiation in comparison to $ALDH^-$ cells (Supplementary Fig. S4A).

Finally, we compared the relative tumorigenicity of DU145 $ALDH^+$ and $ALDH^-$ cells in mice after *in vitro* irradiation. The cells were purified by FACS and irradiated with 0 or 4 Gy of X-ray, embedded in Matrigel, and injected subcutaneously into NMRI *nu/nu* mice (Fig. 3C). Animals alive and tumor-free at the end of the observation period (100 days) were defined as long-term survivors. In contrast to the $ALDH^+$ cells, whose tumor take was not significantly impaired by irradiation, $ALDH^-$ cells had a significantly lower tumor take after irradiation than nonirradiated $ALDH^-$ cells (Fig. 3D). In addition, the difference between relative tumor growth rate of the irradiated $ALDH^+$ cells and $ALDH^-$ cells was significantly higher than for their nonirradiated counterparts (Supplementary Fig. S4B and S4C). It is noteworthy that chemical inhibition of ALDH enzymatic activity with diethylaminobenzaldehyde (DEAB) or galiellalactone resulted in significant increase in cell radiosensitivity *in vitro* (Fig. 3E). Taken together, our results indicate that prostate cancer progenitor cells with a high ALDH activity harbor more radioresistant cells than $ALDH^-$ cell population.

The emergence of radioresistance is associated with a gain of CSC phenotype

To obtain the radioresistant cell sublines, the established prostate cancer cell lines were treated with multiple fractions of 4 Gy of

Published OnlineFirst February 10, 2015; DOI: 10.1158/0008-5472.CAN-14-1924

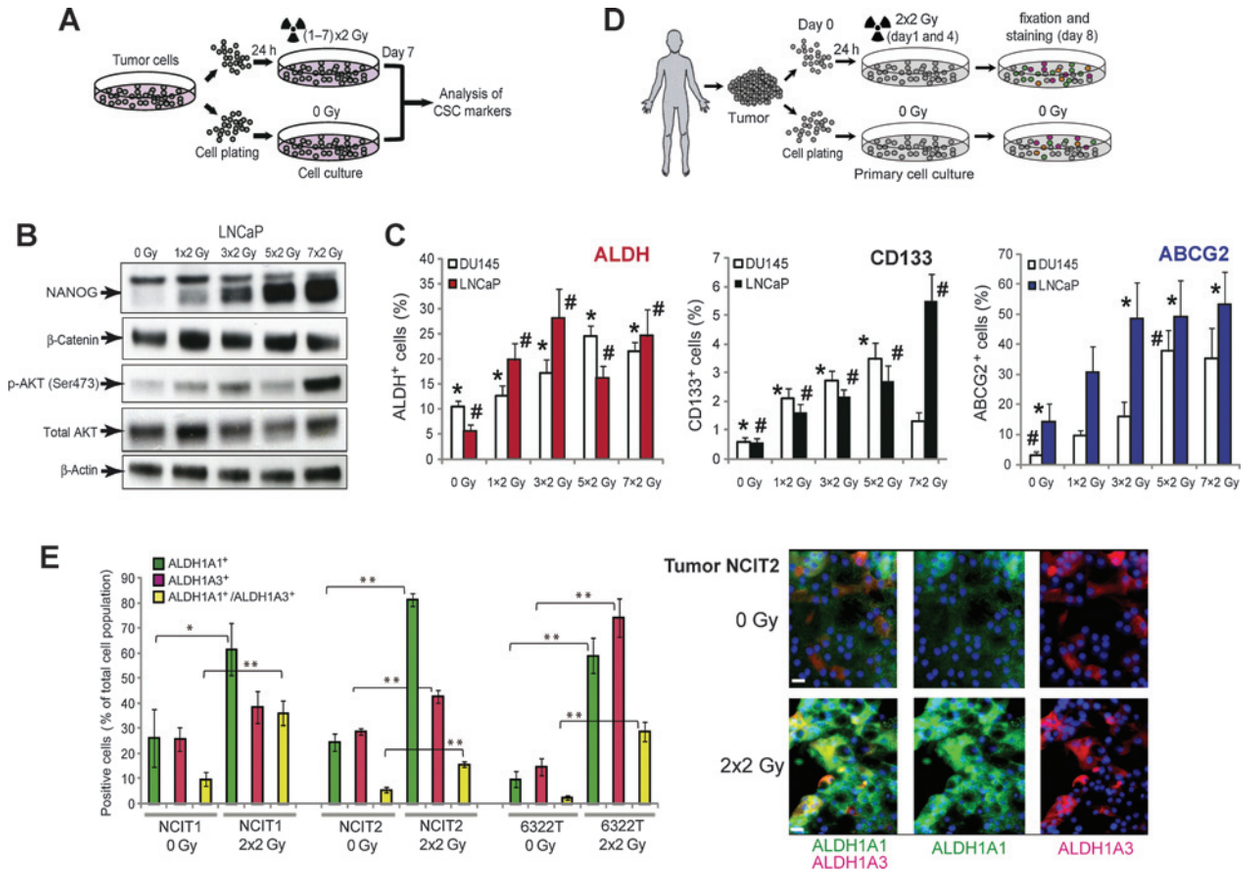

Figure 2.
X-ray irradiation leads to an increase in the progenitor population in prostate cancer cell lines. A, cells were irradiated with the doses indicated, cultured for 7 days, and analyzed by flow cytometry or Western blotting. B, irradiation leads to the upregulation of AKT phosphorylation at Ser473 and to expression of the transcription regulators NANOG and β-catenin. C, flow cytometric analysis of CSC marker expression shows a dose-dependent increase in the number of DU145 and LNCaP cells having a high ALDH activity and expressing CD133 and ABCG2. Error bars, SEM. *, $P < 0.05$; #, $P < 0.05$. D, freshly isolated human prostate cancer specimens were subjected to enzymatic dissociation and single-cell suspension was plated on 96-well clear-bottom collagen I–coated plates at 1,000 cells per well and irradiated with 2 Gy of X-ray the following day and 3 days later. E, four days after irradiation, the number of $ALDH1A1^+$, $ALDH1A3^+$, and $ALDH1A1^+/ALDH1A3^+$ cells was assessed by fluorescent microscopy. For quantification, 200 to 1,000 cells per condition in at least seven randomly selected fields were counted. Error bars, SEM. Scale bar, 30 μm; *, $P < 0.05$.

X-ray irradiation until a total dose of more than 56 Gy was reached (Fig. 4A). The surviving cells showed enhanced radioresistant properties, as it was evaluated in a colony assay. The established radioresistant cell lines maintain their radioresistant status for a few months (Fig. 4B). The radioresistant sublines showed enhanced ALDH activity and elevated expression of stem cell markers such as CD133, ABCG2, CXCR4, and CD44 (Fig. 4C; Supplementary Fig. S5A and S5B).

The radioresistant LNCaP-RR cells maintain their radioresistant properties *in vivo* and have a significantly increased relative tumor growth rate and tumor uptake after *in vitro* irradiation with 4 Gy of X-rays compared with parental, more radiosensitive LNCaP cells. In contrast, LNCaP and LNCaP-RR cells that were not irradiated before injection did not differ in their tumorigenic properties (Fig. 4D and E; Supplementary Fig. S5C and S5D). Consistently with the *in vitro* results, analysis of the xenograft tumors formed by radioresistant tumor cells showed an elevated ALDH activity, increased expression of other stem cell markers such as CD133, NANOG, and BMI1 compared with the xenograft tumors formed by parental LNCaP and DU145 cells (Supplementary Fig. S5E–S5G).

The mechanisms of prostate cancer cell radioresistance

A number of different intrinsic and extrinsic adaptations might confer high cellular radioresistance, including activation of the radiation-induced DNA damage response and enhanced DNA repair capability, increased intracellular defense against ROS, and activation of the survival pathways, including PI3K/AKT signaling (7, 8).

Cellular response to DNA damage is coordinated primarily by two signaling cascades, the ATM–Chk2 and ATR–Chk1 pathways, which are activated by double-strand DNA breaks (DSB) and single-strand DNA breaks (SSB), respectively. After DNA damage by ionizing irradiation, Chk1/2 becomes phosphorylated by ATR/ATM and arrests cell proliferation to allow DNA reparation. Recent studies have also implicated the PI3K/AKT signaling pathway in modulation of DNA damage responses. AKT is activated by DSBs in a DNA protein kinase (DNA-PK) or ATM/ATR-dependent manner and can contribute to the tumor radioresistance by enhancing DNA repair through nonhomologous end joining (NHEJ) and enhanced cell survival (8, 18). We found that radioresistant prostate cancer cell sublines DU145-RR, PC3-RR, and LNCaP-RR have an increased baseline phosphorylation of Chk2 (Thr68) and AKT (Ser473),

Published OnlineFirst February 10, 2015; DOI: 10.1158/0008-5472.CAN-14-1924

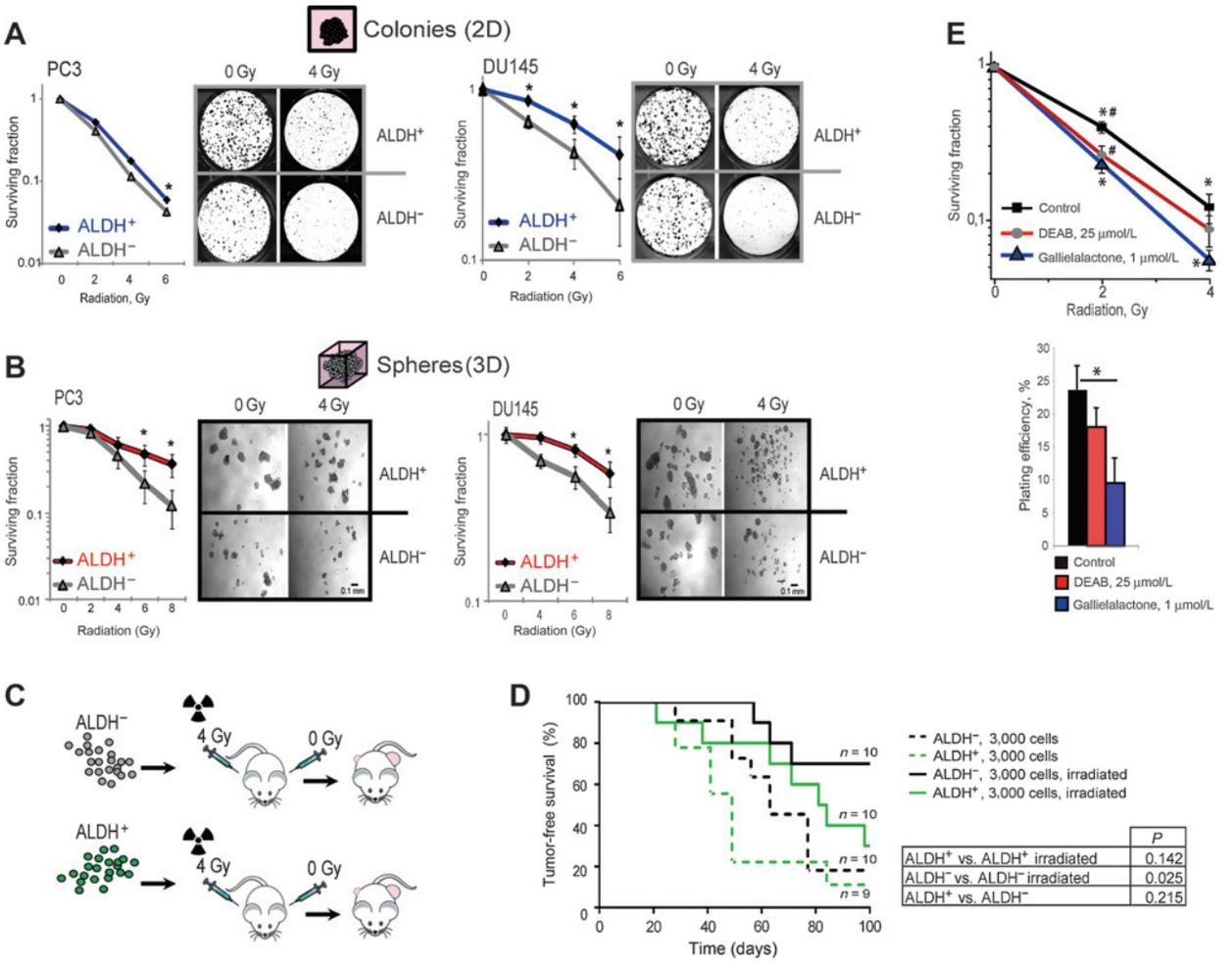

Figure 3.

ALDH$^+$ cancer progenitor cells are resistant to X-ray irradiation. A, susceptibility of ALDH$^+$ and ALDH$^-$ FACS-purified PC3 and DU145 prostate cancer cells to X-ray irradiation was evaluated by a clonogenic cell survival assay. Error bars, SEM. *, $P < 0.05$. B, relative radioresistance of ALDH$^+$ and ALDH$^-$ FACS-purified PC3 and DU145 prostate cancer cells was evaluated by spherogenic cell survival assay. Error bars, SEM. *, $P < 0.05$. C, schematic representation of the setup of *in vivo* study. D, tumor uptake of ALDH$^+$ and ALDH$^-$ DU145 cells irradiated with 4 Gy of X-ray before injection. E, inhibition of ALDH enzymatic activity with 25 μmol/L of DEAB or 1 μmol/L of galiellalactone resulted in significant increase in DU145 cells radiosensitivity. Error bars, SEM. * and #, $P < 0.05$.

suggesting potential molecular mechanisms underlying acquired radioresistance of these tumor cells (Fig. 5A and B).

Another molecular determinant of a high radioresistance of CSC population is an intracellular defense against ROS. Excessive ROS production after irradiation can lead to the cell death via damage of critical macromolecules, including DNA, lipids, and proteins (8). The radioresistant prostate cancer cell sublines DU145-RR and LNCaP-RR have significantly lower baseline level of intracellular ROS as compared with parental cells that together with activated DNA repair can contribute to their higher radioresistance (Fig. 5C; Supplementary Fig. S6A). Chemical inhibition of ALDH enzymatic activity with DEAB had an additive effect with radiation to increase level of intracellular ROS in prostate cancer cells (Fig. 5D).

Microscopic analysis of the FACS-purified ALDH$^+$ and ALDH$^-$ cell populations suggests that the ATM–Chk2 signaling pathway is also highly activated in cells with a high ALDH activity (Fig. 5E; Supplementary Fig. S6B). Furthermore, analysis of the xenograft tumors formed by ALDH$^+$ or ALDH$^-$ cells has shown that ALDH$^+$-derived tumors are enriched for ALDH1A1 cells, have activated PI3K/AKT signaling, and a relatively low level of ROS production (Supplementary Fig. S6C and S6D).

One of the best-characterized chromatin modification events in response to DNA DSB is histone H2A.X phosphorylation by ATM or ATR protein kinase. The phosphorylated form of H2A.X (γ-H2A.X) forms nuclear foci on the sites of DNA damage (19). Residual γ-H2A.X foci measured at 24 hours after irradiation can be used as an indicator of lethal DNA lesions. Analysis of the residual γ-H2A.X foci in the parental and radioresistant LNCaP and DU145 cells 24 hours after irradiation showed that RR cells have a significantly fewer number of foci as compared with the parental cell lines, suggesting that RR cells have more efficient DSB repair after irradiation (Fig. 5F).

It is noteworthy that ALDH$^+$ cell population from DU145 and PC3 cells had significantly fewer number of γ-H2A.X foci at an

Published OnlineFirst February 10, 2015; DOI: 10.1158/0008-5472.CAN-14-1924

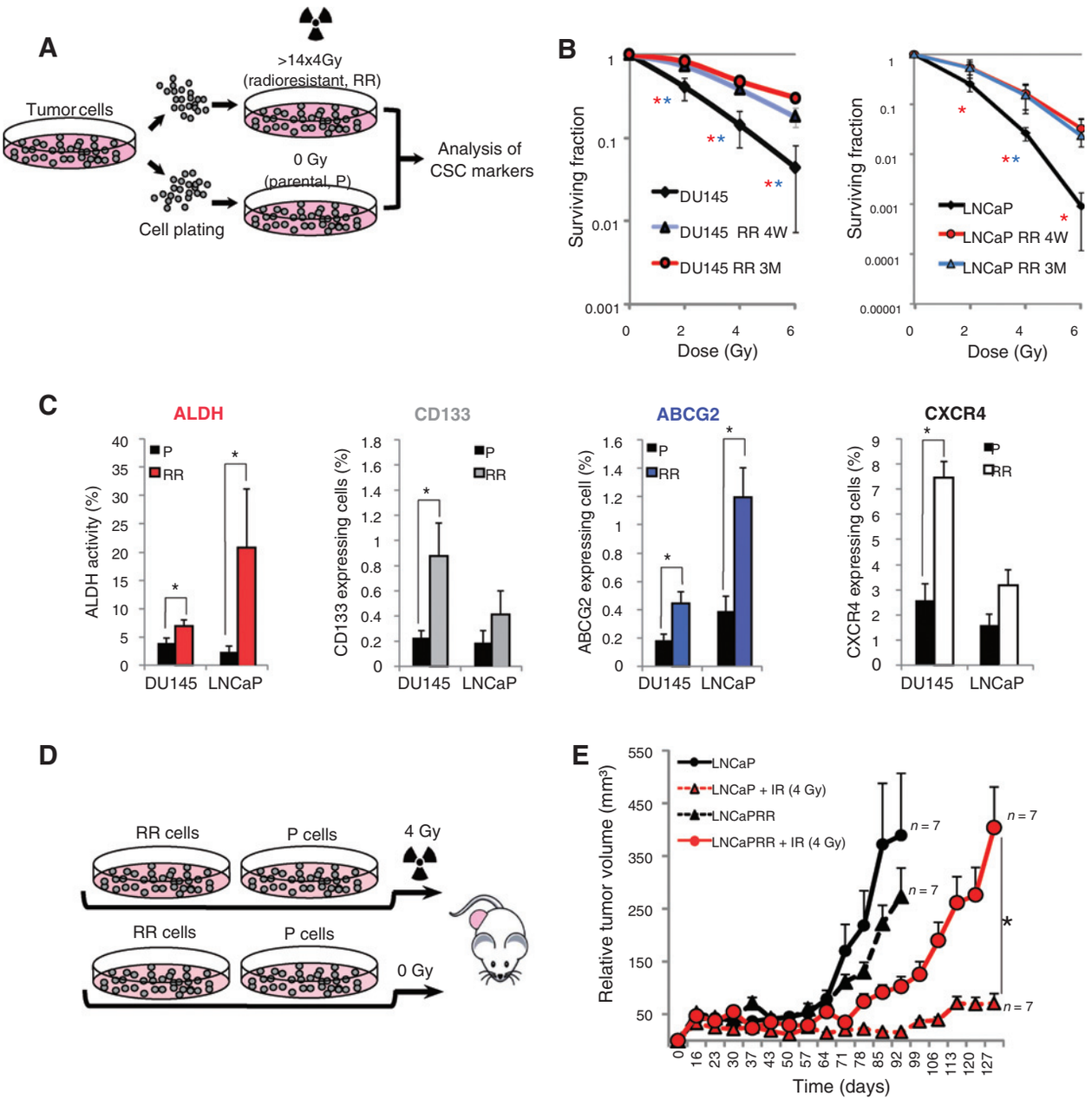

Figure 4.
Characterization of the properties of prostate cancer cells with acquired radioresistance. A, the established prostate cancer cell lines DU145 and LNCaP were treated with multiple fractions of 4 Gy of X-ray irradiation until a total dose of more than 56 Gy was reached. B, cells survived fractionated irradiation with >14 × 4 Gy of X-rays (radioresistant cell subline, RR) showed enhanced radioresistant properties in a colony assay as compared with the parental cells (P). Cells were analyzed 4 weeks (4W) and 3 months (3M) after the last irradiation. Error bars, SD. C, the DU145-RR and LNCaP-RR sublines showed enhanced ALDH activity and elevated expression of stem cell markers, such as CXCR4, ABCG2, and CD133, as compared with the parental cells. The radioresistant cells were analyzed 4 weeks after the last irradiation. Error bars, SEM. *, $P < 0.05$. D, the radioresistant and parental cells were irradiated with 0 or 4 Gy of X-rays, embedded in Matrigel, and injected subcutaneously into NMRI *nu/nu* mice (10^6 cells per injection site). E, relative tumor growth of LNCaP-RR and LNCaP cells. Error bars, SEM. *, $P < 0.05$.

early time point of 1 hour after irradiation and significantly less residual γ-H2AX foci 24 hours after irradiation as compared with $ALDH^-$ cells. The results of this experiment demonstrated that a lower number of the residual γ-H2A.X foci in $ALDH^+$ cells can be attributed to both lower level of DNA double-strand breaks and more efficient DNA repair (Fig. 5G).

A number of recent reports suggest that hypoxic niches directly protect CSCs by lack of oxygen and support CSC maintenance and expansion, at least in part, through the activation of the hypoxia-inducible factor (HIF) signaling pathway (20, 21). Expression of the stem cell markers *ALDH1A1*, *CD44*, and *PROM1* (CD133) has a tendency toward co-occurrence with HIF1α expression in

Published OnlineFirst February 10, 2015; DOI: 10.1158/0008-5472.CAN-14-1924

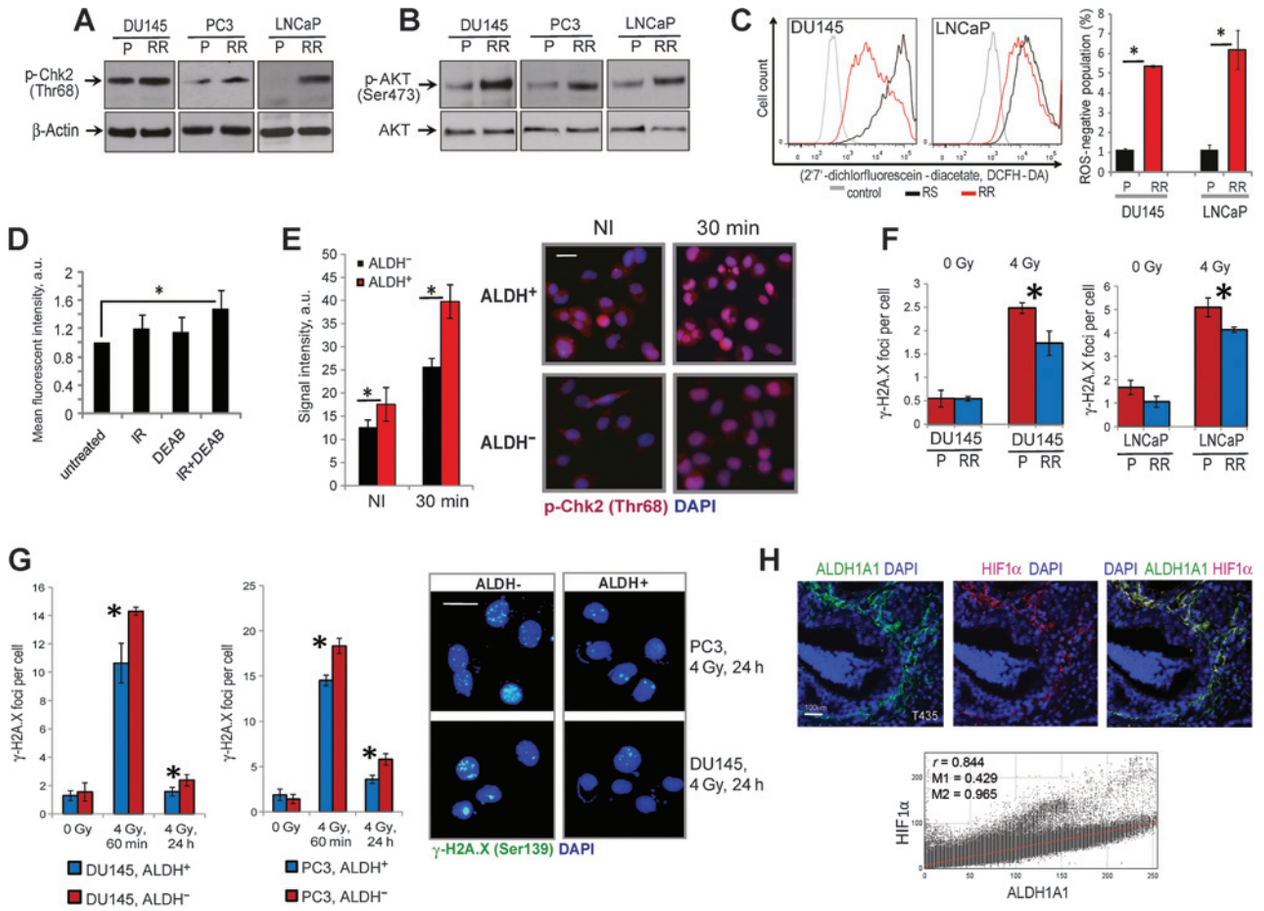

Figure 5.

The mechanisms of prostate cancer cell radioresistance. A, radioresistant (RR) prostate cancer cells have an increased level of Chk2 phosphorylation (Thr68). B, phosphorylation level of AKT (Ser473) is increased in radioresistant cells. C, radioresistant prostate cancer cells have low intracellular level of ROS. Radioresistant cells were analyzed 4 weeks after the last irradiation. Error bars, SEM. *, $P < 0.05$. D, chemical inhibition of ALDH enzymatic activity with 25 μmol/L of DEAB had an additive effect with radiation to increase level of intracellular ROS in prostate cancer cells. IR, irradiation with 4 Gy of X-rays. *, $P < 0.05$. E, immunofluorescent analysis of Chk2 phosphorylation (Thr68) in FACS-sorted ALDH$^+$ and ALDH$^-$ cells without irradiation (NI) and 30 minutes after irradiation with 4 Gy of X-ray. Scale bars, 30 μm. F, analysis of the residual γ-H2A.X foci in the parental and radioresistant LNCaP and DU145 cells 24 hours after irradiation. Error bars, SEM. *, $P < 0.05$. G, a number of γ-H2A.X foci in ALDH$^-$ and ALDH$^+$ cells 60 min and 24 hours after irradiation. Error bars, SEM. Scale bar, 30 μm. *, $P < 0.05$. H, representative image of immunofluorescent staining of ALDH1A1 and HIF1α in prostate tumors. Three formalin-fixed, paraffin-embedded prostate tumor specimens were analyzed. Scale bar, 100 μm. The Pearson correlation coefficient (*r*) and Mander correlation coefficients (*M*) were analyzed using Fiji software.

prostate tumor specimens (Supplementary Fig. S6E). Moreover, IHC analysis revealed an overlap in ALDH1A1 and HIF1α expression in primary human prostate tumors, suggesting that a subset of ALDH$^+$ cells might be radioresistant *in vivo* due to their protection from radiation damage by hypoxia (Fig. 5H; Supplementary Fig. S6F and S6G).

Comparative gene expression profiles of prostate cancer progenitor and radioresistant cells

By using a global gene expression profiling, we performed a more comprehensive analysis of the molecular pathways that are similarly activated in DU145 ALDH$^+$ and DU145-RR cells. We performed pathway enrichment analysis using the PANTHER pathway tool to highlight shared intracellular signaling mechanisms and found that 36% (9 of 25) of the molecular pathways overrepresented in DU145 ALDH$^+$ cell population comprise 47% (9 of 19) of the pathways, which were also overrepresented in DU145-RR cells (Supplementary Fig. S7A). The signaling axes that are commonly overrepresented in ALDH$^+$ and DU145-RR cells include already known mechanisms regulating CSC population, such as WNT/cadherin, heterotrimeric G-protein, TGFβ, and integrin signaling pathways, angiogenesis and inflammation but also signaling axes that were not previously known to be associated with CSC and radioresistance, such as the Alzheimer disease–presenilin pathway, Huntington disease, and oxytocin receptor–mediated signaling (Supplementary Fig. S7B).

WNT/β-Catenin signaling plays a role in the maintenance of radioresistant ALDH$^+$ prostate cancer cells

A number of studies indicate that WNT signaling plays a central role in the maintenance of the CSC populations of various tumor types (22). Activation of the canonical WNT signaling pathway is

Published OnlineFirst February 10, 2015; DOI: 10.1158/0008-5472.CAN-14-1924

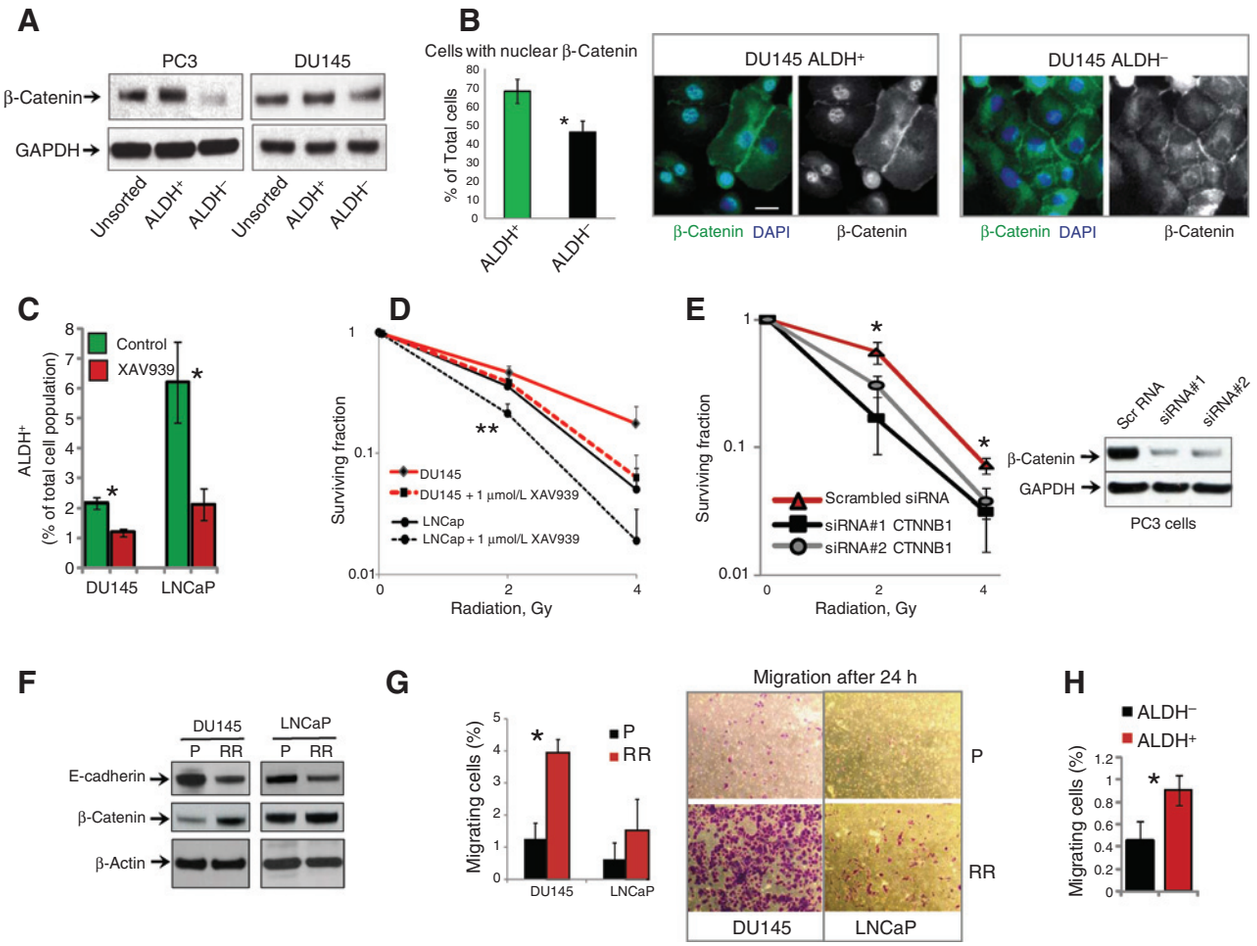

Figure 6.
Activation of the WNT signaling pathway in ALDH$^+$ cell population and radioresistant prostate cancer cells. A, Western blot analysis of the FACS-purified ALDH$^+$ and ALDH$^-$ cells showed a high level of β-catenin expression in ALDH$^+$ cell population. B, immunofluorescent analysis of the intracellular distribution of β-catenin in ALDH$^+$ and ALDH$^-$ cell subsets. Error bars, SEM. Scale bar, 30 μm. *, $P < 0.05$. C, the chemical inhibition of the WNT pathway by XAV939 antagonist led to significant inhibition of the ALDH$^+$ population in the prostate cancer cells. The cells were serum-starved in DMEM with 1% FBS for 24 hours followed by treatment with XAV939 antagonist at concentration 1 μmol/L for 3 days. Error bars, SEM. Scale bar, 30 μm. *, $P < 0.05$. D, the inhibition of the WNT signaling pathway with XAV939 inhibitor at concentration 1 μmol/L resulted in significant increase in radiosensitivity of LNCaP and DU145 cells. Error bars, SEM. **, $P < 0.01$. E, knockdown of β-catenin mediated by siRNA led to a significant prostate cancer cells radiosensitization. Error bars, SEM. *, $P < 0.05$. F, level of E-cadherin and β-catenin expression in the radioresistant (RR) and parental DU145 and LNCaP cells. G, transwell migration assay showed that radioresistant cells have an increased migratory potential relative to the parental cells. Radioresistant cells were used 4 weeks after the last irradiation. Error bars, SD. *, $P < 0.05$. H, ALDH$^+$ and ALDH$^-$ cells isolated by FACS from DU145 cells were analyzed for their migratory properties in a transwell migration assay. Error bars, SEM. *, $P < 0.05$.

associated with the stabilization and accumulation of nuclear β-catenin, which interact with T-cell factor/lymphoid-enhancing factor-1 (TCF/LEF) transcription factors to promote gene expression. Numerous experiments have demonstrated an interplay of cadherin-mediated cell adhesion and WNT signaling in regulation of EMT, therapy resistance, and metastasis development (22–24). Western blot analysis of the FACS-purified ALDH$^+$ and ALDH$^-$ cells showed a high level of β-catenin expression in ALDH$^+$ cell population (Fig. 6A). In addition, analysis of the intracellular distribution of β-catenin in ALDH$^+$ and ALDH$^-$ cell subsets showed that ALDH$^+$ cells have an increased nuclear β-catenin level that indicates the activation of the WNT signaling pathway (Fig. 6B). Consistently with the results of Western blot analysis and immunofluorescent staining, the chemical inhibition of the WNT pathway by tankyrase inhibitor XAV939, which stimulates β-catenin degradation led to significant inhibition of the ALDH$^+$ population in LNCaP and DU145 cells (Fig. 6C; ref. 25). Moreover, WNT inhibition by XAV939 had a radiosensitization effect for LNCaP and DU145 prostate cancer cells (Fig. 6D). Knockdown of β-catenin mediated by siRNA resulted in a significant increase in PC3 prostate cancer cells radiosensitivity as it was demonstrated by a clonogenic cell survival assay (Fig. 6E).

WNT and TGFβ signaling, which are overrepresented in both radioresistant prostate cancer cells and ALDH$^+$ tumor progenitor population are potent inducers of EMT, which plays a critical role in the maintenance and generation of CSCs (26–28). Moreover, recent studies have shown that CSCs population surviving chemo- and radiotherapy have the phenotypic hallmarks of EMT (29–31).

Published OnlineFirst February 10, 2015; DOI: 10.1158/0008-5472.CAN-14-1924

Emergence of radioresistance resulted in reversion from the epithelioid shape of the parental DU145 and LNCaP cells to the stellate shape observed during EMT (Supplementary Fig. S8A). Analysis of the expression of EMT markers in the radioresistant and parental prostate cancer cell lines showed that acquired radioresistance is associated with the loss of E-cadherin expression and increased expression of β-catenin (Fig. 6F). Western blot analysis showed an induction of β-catenin expression after irradiation (Supplementary Fig. S8B). The results of the wound-healing and Boyden chamber–based assays demonstrated a high migratory potential of the radioresistance prostate cancer cells (Fig. 6G, Supplementary Fig. S8C). Finally, we analyzed the migratory potential of $ALDH^+$ and $ALDH^-$ populations isolated from DU145 and LNCaP cell lines and found that $ALDH^+$ cells have higher migratory properties as compared with $ALDH^-$ cell population (Fig. 6H; Supplementary Fig. S8D).

Activation of the WNT/β-catenin signaling pathway by glycogen synthase kinase (GSK-3) inhibitor LiCl or stimulation of β-catenin degradation by XAV939 led to an increase or downregulation of ALDH1A1 protein expression, respectively (Supplementary Fig. S9A). Knockdown of β-catenin mediated by siRNA transfection strongly decreased protein expression of ALDH1A1 (Fig. 7A). A correlation between the protein expression level of ALDH1A1 and β-catenin in prostate cancer cells suggested that the WNT pathway could regulate ALDH1A1 level directly through β-catenin/TCF-dependent transcription or indirectly via different β-catenin/TCF target genes. Analysis of the *ALDH1A1* gene promoter revealed two core β-catenin/TCF–binding sites CTTTG A/T A/T (Fig. 7B). To determine whether β-catenin/TCF transcriptional complex can bind to the *ALDH1A1* promoter, a chromatin immunoprecipitation (ChIP) assay was performed. The cross-linked DNA–protein complexes were immunoprecipitated either with anti-β-catenin or with anti-TCF4 antibodies. PCR amplification was performed using primers flanking two putative β-catenin/TCF-binding sites named ALDH1A1(i) and ALDH1A1(ii) (Fig. 7B). The results of ChIP analysis showed that *ALDH1A1* promoter DNA was precipitated with both, anti-β-catenin or with anti-TCF4 antibodies, suggesting a direct regulation of *ALDH1A1* expression by β-catenin/TCF transcriptional complex (Fig. 7C). To analyze the transcriptional regulation of ALDH1A1, we used reporter system where luciferase gene expression is regulated by an endogenous *ALDH1A1* gene promoter. The results of a luciferase reporter assay showed that XAV939 or siRNA-mediated downregulation of the endogenous β-catenin or overexpression of wild-type β-catenin led to a significant decrease or upregulation of *ALDH1A1* transcription, respectively (Fig. 7D, Supplementary Fig. S9B–S9D). Moreover, expression of *ALDH1A1* and *ALDH6A1* genes has a tendency toward co-occurrence with *CTNNB1* (β-catenin) in prostate tumor specimens (Fig. 7E). IHC analysis showed an overlap in ALDH1A1- and β-catenin–positive cell populations in primary prostate tumor cells (Fig. 7F). These data suggest overlapping signaling mechanisms that govern tumor-initiating properties, EMT, and radioresistance (Fig. 7G).

Discussion

Radiation therapy is one of the mainstays of curative treatment of clinically localized prostate carcinoma. However, one of the main obstacles to external beam radiotherapy is a limited dose that can be delivered to the tumor due to normal tissue tolerance (32). From a clinical point of view, a patient suffering from cancer can be only cured if all CSCs are eradicated (6). Recent study has shown that the most lethal metastatic prostate cancer can potentially arise from a single CSC (33). Therefore, efficient anticancer therapy is expected to target all CSCs. The CSC concept has been elevated to a higher level of clinical significance by a large number of *in vitro* investigations showing differences in radiosensitivity of putative CSC and non-CSC populations. Possible relative radioresistance of CSCs has been explained by their quiescent status, activated DNA checkpoints, high free radical scavenger level, activation of the antiapoptotic signaling pathways, and by extrinsic contribution of the tumor microenvironment (7, 8).

Currently, tumor response in many of clinical studies is determined by volume-related endpoints, such as tumor regression or growth delay, that may not always correlate with local tumor control (34, 35). The relative frequency of CSC is highly variable between different tumor types, and even among tumors of the same clinical entity, ranging from a very small population (<1%) as in acute myeloid leukemia or pancreatic cancer, up to 20% to 40% as in some brain, bladder, colorectal cancer, and melanoma. Therefore, therapies that eradicate tumor-initiating cells may not always result in tumor shrinkage (36). On the other hand, common anticancer therapies, including chemotherapy and radiotherapy, eradicate the bulk of tumor cells and lead to decrease in tumor volume but not always targeting the entire CSC population (34, 35, 37, 38). Prediction of the probability of successful treatment is of high importance for the individualization of prostate cancer treatment. The current prostate cancer risk stratification system, which is based on prostate-specific antigen (PSA), T stage, and Gleason score and used for treatment decision-making, is of great clinical value, yet not perfect and there remains a lack of reliable indicators of patients' response to radiotherapy (39, 40).

Retrospective clinical studies for the different types of cancer have shown that analysis of CSC-specific markers in pretherapeutic biopsies might be an important tool for prediction of radiotherapy outcome and appropriate treatment selection (9). Despite a few shortcomings of these studies, including a low number of the patients that hamper multivariate analysis and the usage of volume-related endpoint parameters such as tumor regression or growth delay, as well as the absence of the functional characterization of the marker-positive cells, these studies paved an avenue for future biomarker development. Recent analysis of the presence and clinical significance of $ALDH^+$ populations in prostate cancer specimens demonstrated that ALDH1 expression was significantly increased in cancers in advanced stage with high Gleason scores and was associated with poor survival in hormone-naïve patients. This clinical study used a large cohort of multistage prostate cancer specimens and demonstrated that analysis of ALDH1A1 expression might help improve risk stratification in patients with prostate cancer (41).

In the current study, we found that prostate cancer progenitor cells with high ALDH activity ($ALDH^+$ cells) are more radioresistant than $ALDH^-$ cells, and inhibition of ALDH activity radiosensitizes prostate cancer cells. Our data demonstrated that resistance of $ALDH^+$ cells to radiotherapy might be conferred by more efficient mechanisms of DNA repair and ROS scavenging as well as activation of the cell survival pathways, such as WNT/β-catenin, PI3K/AKT, and integrin signaling pathways. Primary human prostate tumors consist of $ALDH1A1^+$ cells with a high level of expression of HIF1α, which has been suggested as a master regulator of CSCs and an endogenous marker of tumor hypoxia

Published OnlineFirst February 10, 2015; DOI: 10.1158/0008-5472.CAN-14-1924

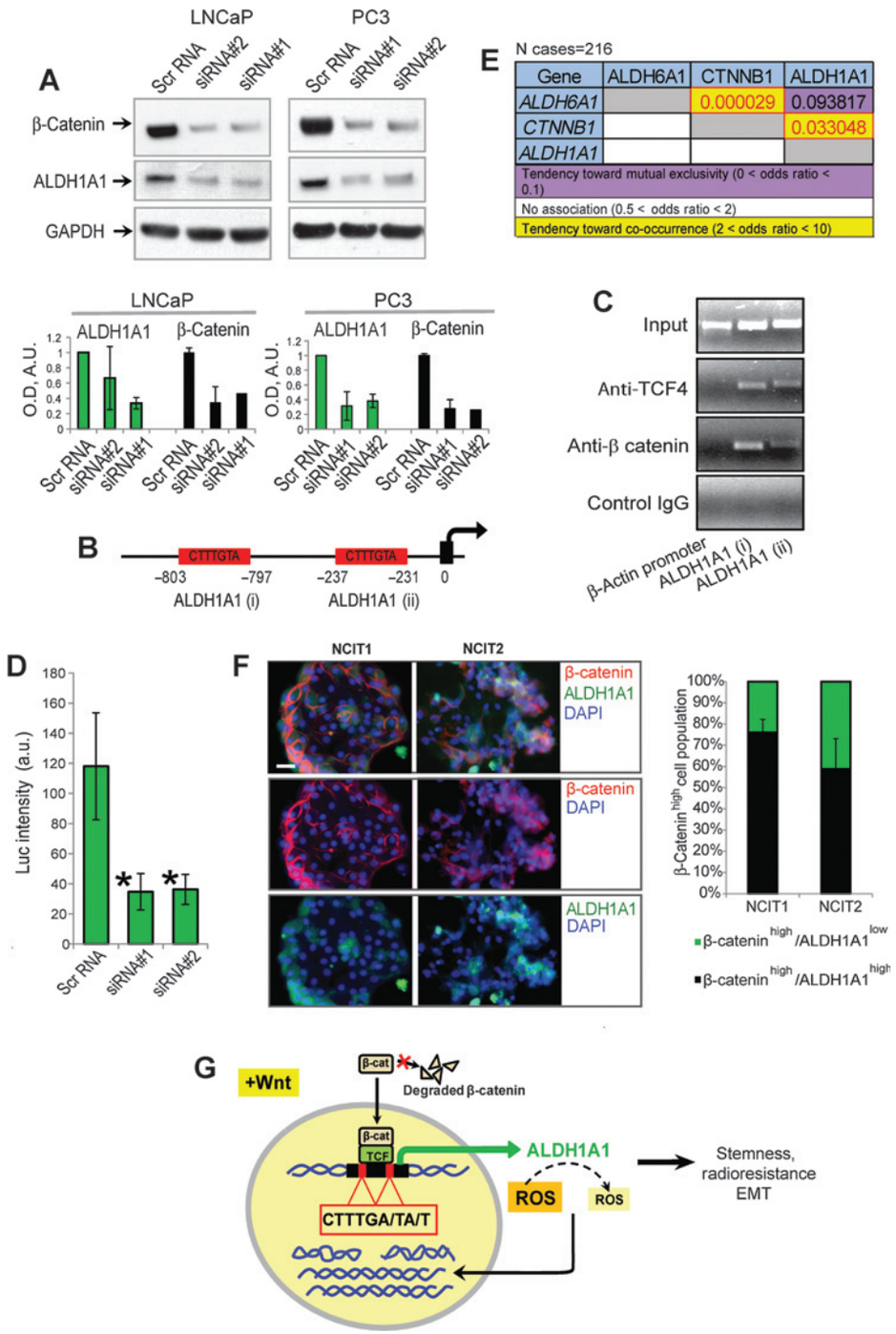

Figure 7.
WNT/β-catenin–dependent regulation of the ALDH1A1 protein expression. A, knockdown of β-catenin mediated by siRNA transfection strongly decreased protein expression of ALDH1A1. The densitometry of Western blot bands was performed using ImageJ software based on the analysis of 2 (LNCaP) or 4 (PC3) biologic replicates of Western blotting. OD, optical density; AU, arbitrary units. B, two core β-catenin/TCF–binding sites CTTTG A/T A/T within the *ALDH1A1* gene promoter. C, the results of ChIP analysis showed that *ALDH1A1* promoter binds to β-catenin/TCF4 transcription complex. D, the results of a luciferase reporter assay where luciferase gene expression is regulated by an endogenous *ALDH1A1* gene promoter showed that siRNA-mediated downregulation of the endogenous β-catenin significantly decreases *ALDH1A1* transcription. Error bars represent SD. *, $P < 0.05$. E, expression of ALDH1A1 and ALDH6A1 has a tendency toward co-occurrence with expression of CTNNB1 (β-catenin) in prostate tumor specimens. Data are based on the Taylor study (14). Data were analyzed using cBioPortal for Cancer Genomics. $P < 0.05$, as derived via the Fisher exact test, are outlined in red. *P* values are not adjusted for FDR. F, representative images of IHC analysis showing expression of ALDH1A1 and β-catenin in primary prostate tumor cells. Error bars represent SEM. Scale bar, 50 μm. G, model depicting the proposed mechanism of regulation of cell radioresistance by the *WNT*/β-catenin/ALDH1A1 signaling pathway. Activation of the WNT signaling pathway leads to an increase of β-catenin/TCF4–dependent transcription of the *ALDH1A1* gene. ALDH is required to maintain ROS level sufficiently low to prevent irradiation-induced oxidative DNA damage. ALDH activity is indicative of radioresistant prostate progenitor cells with activation of EMT and high migratory potential.

and associated radioresistance (20, 42–44). Importantly, irradiated ALDH$^+$ cells maintain their tumorigenic properties *in vivo*, suggesting that ALDH$^+$ prostate cancer cells are a cell population that may be able to regrow after radiotherapy.

Our results are in agreement with a recent study on breast cancer cells from Duru and colleagues who showed that HER2$^+$ cells isolated from HER2-negative breast cancer cells are radioresistant and ALDH-positive (45). Another study of Wang and colleagues demonstrated that ALDH inhibition by disulfiram (DSF) effectively depleted pre-existing and radiation-induced breast CSCs (46). A notable study by Mao and colleagues demonstrated that highly radioresistant mesenchymal glioma stem cells are maintained by activated glycolytic metabolism involving ALDH1A3, and inhibition of ALDH1 reverses the radioresistant phenotype of CSCs (47). These data and our results are in agreement with recently published study from Pate and colleagues showing that

WNT signaling drives a glycolytic metabolism and stimulates HIF1α stabilization in colon cancer (48).

We found that chemical and genetic inhibition of the WNT/β-catenin signaling pathway inhibits $ALDH^+$ cell population and radiosensitizes prostate cancer cells. In the present study, we identified a new link between tumor radioresistance and tumorigenicity. We report for the first time that the WNT pathway directly regulates ALDH1A1 level through β-catenin/TCF-dependent transcription, and expression of ALDH1A1 co-occurs with expression of β-catenin in human prostate tumors. Recent clinical studies of WNT targeting compounds for the treatment of various solid tumors, including OMP-54F28 (NCT01608867, NCT02069145, NCT02092363, NCT02050178), OMP-18R5 (NCT01345201), PRI-724 (NCT01606579, NCT01302405), and LGK974 (NCT01351103) could pave the way to improve the effectiveness of cancer treatment by combination of radiotherapy with $ALDH^+$ cell targeting treatment.

Consistent with our results for a high relative radioresistance of $ALDH^+$ cells, we found that $ALDH^+$ cell population is enriched within prostate cancer cells with acquired radioresistance. Whole-genome gene expression profiling revealed a few common signaling pathways that link $ALDH^+$ progenitors and RR cells and include WNT/β-catenin, G-protein–coupled receptor, TGFβ, and integrin signaling pathways. Our data suggest that emergence of radioresistance by prostate cancer cells is associated with gaining of EMT features and migratory behavior and that both $ALDH^+$ cell population and RR prostate cancer cells have a high migratory potential. This finding is in agreement with a number of recent studies suggesting that gain of the EMT features contributes to radioresistance (47, 49, 50). Thus, targeting ALDH might provide a new approach to improve the efficacy of prostate cancer radiotherapy.

Taken together, our results indicate that $ALDH^+$ tumor–initiating cells can potentially contribute to prostate tumor radioresistance, and therapies that specifically target this cell population might be a biologically driven strategy to enhance the efficacy of radiotherapy. Further functional radiobiologic assays and analysis of the expression level of ALDH1 in a retrospective cohort of patients who were treated with radiotherapy may lead to the development of novel predictive biomarker for radiation response in prostate cancer.

Disclosure of Potential Conflicts of Interest

M. Wirth has honoraria from the speakers' bureau of Apogepha, Bayer, Sanofi-Aventis, Orion, and Pfizer and is a consultant/advisory board member of Bayer, Janssen, Merck, Takeda, Roche, Apogepha, Dendreon, Farco-Pharma, Ferring, Ipsen, and Janssen-Cilag. No potential conflicts of interest were disclosed by the other authors.

Authors' Contributions

Conception and design: M. Cojoc, C. Peitzsch, L.A. Kunz-Schughart, M.P. Wirth, M. Krause, A. Dubrovska

Development of methodology: M. Cojoc, C. Peitzsch, I. Kurth, F. Trautmann, L.A. Kunz-Schughart, A. Dubrovska

Acquisition of data (provided animals, acquired and managed patients, provided facilities, etc.): M. Cojoc, C. Peitzsch, G.D. Telegeev, E.A. Stakhovsky, J.R. Walker, K. Simin, S. Lyle

Analysis and interpretation of data (e.g., statistical analysis, biostatistics, computational analysis): M. Cojoc, C. Peitzsch, I. Kurth, F. Trautmann, J.R. Walker, M.P. Wirth, A. Dubrovska

Writing, review, and/or revision of the manuscript: M. Cojoc, C. Peitzsch, L.A. Kunz-Schughart, S. Fuessel, K. Erdmann, M.P. Wirth, M. Krause, M. Baumann, A. Dubrovska

Administrative, technical, or material support (i.e., reporting or organizing data, constructing databases): M. Cojoc, L.A. Kunz-Schughart, S. Lyle, A. Dubrovska

Study supervision: A. Dubrovska

Acknowledgments

The authors thank Vasyl Lukiyanchuk for his assistance with gene expression data and Celigo image analysis, Dr. Michael Muders for evaluation of the histologic slides, and Dr. Sandra Hering for her support with microsatellite polymorphism analysis.

Grant Support

This work was supported by BMBF grants (ZIK OncoRay) to A. Dubrovska, M. Baumann, M. Krause and by the German Cancer Consortium (DKTK).

The costs of publication of this article were defrayed in part by the payment of page charges. This article must therefore be hereby marked *advertisement* in accordance with 18 U.S.C. Section 1734 solely to indicate this fact.

Received June 30, 2014; revised November 20, 2014; accepted December 31, 2014; published OnlineFirst February 10, 2015.

References

1. Horwich A, Parker C, Reijke T, Kataja V. Prostate cancer: ESMO Clinical Practice Guidelines for diagnosis, treatment and follow-up. Ann Oncol 2013;Suppl 6:vi106–14.
2. Mohler JL, Kantoff PW, Armstrong AJ, Bahnson RR, Cohen M, D'Amico AV, et al. Prostate cancer, version 1.2014. J Natl Compr Canc Netw 2013;11:1471–9.
3. Zietman AL, Bae K, Slater JD, Shipley WU, Efstathiou JA, Coen JJ, et al. Randomized trial comparing conventional-dose with high-dose conformal radiation therapy in early-stage adenocarcinoma of the prostate: long-term results from Proton Radiation Oncology Group/American College of Radiology 95-09. J Clin Oncol 2010;28:1106–11.
4. Pahlajani N, Ruth KJ, Buyyounouski MK, Chen DYT, Horwitz EM, Hanks GE, et al. Radiotherapy doses of 80 Gy and higher are associated with lower mortality in men with gleason score 8 to 10 prostate cancer. Int J Radiat Oncol 2012;82:1949–56.
5. Johansson S, Aström L, Sandin F, Isacsson U, Montelius A, Turesson I. Hypofractionated proton boost combined with external beam radiotherapy for treatment of localized. Prostate Cancer 2012;2012:654861.
6. Baumann M, Krause M, Hill R. Exploring the role of cancer stem cells in radioresistance. Nat Rev Cancer 2008;8:545–54.
7. Peitzsch C, Kurth I, Kunz-Schughart L, Baumann M, Dubrovska A. Discovery of the cancer stem cell related determinants of radioresistance. Radiother Oncol 2013;108:378–87.
8. Bütof R, Dubrovska A, Baumann M. Clinical perspectives of cancer stem cell research in radiation oncology. Radiother Oncol 2013;108:388–96.
9. Hu Y, Smyth GK. ELDA: extreme limiting dilution analysis for comparing depleted and enriched populations in stem cell and other assays. J Immunol Methods 2009;347:70–8.
10. Collins AT, Berry PA, Hyde C, Stower MJ, Maitland NJ. Prospective identification of tumorigenic prostate cancer stem cells. Cancer Res 2005;65:10946–51.
11. Patrawala L, Calhoun-Davis T, Schneider-Broussard R, Tang D.G. Hierarchical organization of prostate cancer cells in xenograft tumors: the CD44+α2β1+ cell population is enriched in tumor-initiating cells. Cancer Res 2007;67:6796–805.
12. Dubrovska A, Elliott J, Salamone RJ, Kim S, Aimone LJ, Walker JR, et al. Combination therapy targeting both tumor-initiating and differentiated cell populations in prostate carcinoma. Clin Cancer Res 2010;16:5692–702.

13. Tang DG, Patrawala L, Calhoun T, Bhatia B, Choy G, Schneider-Broussard R, et al. Prostate cancer stem/progenitor cells: identification, characterization, and implications. Mol Carcinog 2007;46:1–14.
14. Taylor BS, Schultz N, Hieronymus H, Gopalan A, Xiao Y, Carver BS, et al. Integrative genomic profiling of human prostate cancer. Cancer Cell 2010;18:11–22.
15. Dubrovska A, Kim S, Salamone RJ, Walker JR, Maira SM, García-Echeverría C, et al. The role of PTEN/Akt/PI3K signaling in the maintenance and viability of prostate cancer stem-like cell populations. Proc Natl Acad Sci 2009;106:268–73.
16. Asuthkar S, Gondi CS, Nalla AK, Velpula KK, Gorantla B, Rao JS. Urokinase-type plasminogen activator receptor (uPAR)-mediated regulation of WNT/β-catenin signaling is enhanced in irradiated medulloblastoma cells. J Biol Chem 2012;287:20576–89.
17. Ghisolfi L, Keates AC, Hu X, Lee D, Li CJ. Ionizing radiation induces stemness in cancer cells. PLoS One 2013;7:e43628.
18. Xu N, Lao Y, Zhang Y, Gillespie DA. Akt: a double-edged sword in cell proliferation and genome stability. J Oncol 2012;2012:951724.
19. Sharma A, Singh K, Almasan A. Histone H2AX phosphorylation: a marker for DNA damage. In:Bjergbæk L, editor. DNA repair protocols. New York: Humana Press; 2012. p. 613–26.
20. Diehn M, Cho RW, Lobo NA, Kalisky T, Dorie MJ, Kulp AN, et al. Association of reactive oxygen species levels and radioresistance in cancer stem cells. Nature 2009;458:780–83.
21. Li Z, Bao S, Wu Q, Wang H, Eyler C, Sathornsumetee S, et al. Hypoxia-inducible factors regulate tumorigenic capacity of glioma stem cells. Cancer Cell 2009;15:501–13.
22. Holland JD, Klaus A, Garratt AN, Birchmeier W. Wnt signaling in stem and cancer stem cells. Curr Opin Cell Biol 2013;25:254–64.
23. Heuberger J, Birchmeier W. Interplay of cadherin-mediated cell adhesion and canonical Wnt signaling. Cold Spring Harb Perspect Biol 2010;2: a002915.
24. Krasnapolski A, Todaro MB, de Kier Joffe E. Is the epithelial-to-mesenchymal transition clinically relevant for the cancer patient? Curr Pharm Biotechnol 2011;2:1891–9.
25. Jho EH, Zhang T, Domon C, Joo CK, Freund JN, Costantini F. Wnt/beta-catenin/Tcf signaling induces the transcription of Axin2, a negative regulator of the signaling pathway. Mol Cell Biol 2002;22:1172–83.
26. Mani SA, Guo W, Liao MJ, Eaton EN, Ayyanan A, Zhou AY, et al. The epithelial-mesenchymal transition generates cells with properties of stem cells. Cell 2008;133:704–15.
27. McDonald OG, Wu H, Timp W, Doi A, Feinberg AP. Genome-scale epigenetic reprogramming during epithelial-to-mesenchymal transition. Nat Struct Mol Biol 2011;18:867–74.
28. Tang DG. Understanding cancer stem cell heterogeneity and plasticity. Cell Res 2012;22:457–72.
29. Marie-Egyptienne DT, Lohse I, Hill RP. Cancer stem cells, the epithelial to mesenchymal transition (EMT) and radioresistance: potential role of hypoxia. Cancer Lett 2013;341:63–72.
30. Tiwari N, Gheldof A, Tatari M, Christofori G. EMT as the ultimate survival mechanism of cancer cells. Semin Cancer Biol 2012;22:194–207.
31. Theys J, Jutten B, Habets R, Paesmans K, Groot AJ, Lambin P, et al. E-Cadherin loss associated with EMT promotes radioresistance in human tumor cells. Radiother Oncol 2011;99:392–7.
32. Bonkhoff H. Factors implicated in radiation therapy failure and radiosensitization of prostate cancer. Prostate Cancer 2012;2012:593241.
33. Liu W, Laitinen S, Khan S, Vihinen M, Kowalski J, Yu G, et al. Copy number analysis indicates monoclonal origin of lethal metastatic prostate cancer. Nat Med 2009;15:559–65.
34. Baumann M, Krause M, Zips D, Eicheler W, Dörfler A, Ahrens J, et al. Selective inhibition of the epidermal growth factor receptor tyrosine kinase by BIBX1382BS and the improvement of growth delay, but not local control, after fractionated irradiation in human FaDu squamous cell carcinoma in the nude mouse. Int J Radiat Biol 2003;79: 547–59.
35. Krause M, Prager J, Zhou X, Yaromina A, Dörfler A, Eicheler W, et al. EGFR-TK inhibition before radiotherapy reduces tumour volume but does not improve local control: differential response of cancer stem cells and nontumourigenic cells? Radiother Oncol 2007;83:316–25.
36. Baccelli I, Trumpp A. The evolving concept of cancer and metastasis stem cells. J Cell Biol 2012;198:281–93.
37. Liu S, Wicha MS. Targeting breast cancer stem cells. J Clin Oncol 2010;28:4006–12.
38. Monetti F, Casanova S, Grasso A, Cafferata MA, Ardizzoni A, Neumaier CE. Inadequacy of the new Response Evaluation Criteria in Solid Tumors (RECIST) in patients with malignant pleural mesothelioma: report of four cases. Lung Cancer 2004;43:71–4.
39. Rodrigues G, Warde P, Pickles T, Crook J, Brundage M, Souhami L, et al. Pretreatment risk stratification of prostate cancer patients: a critical review. Can Urol Assoc J 2012;6:121–7.
40. Sutcliffe P, Hummel S, Simpson E, Young T, Rees A, Wilkinson A , et al. Use of classical and novel biomarkers as prognostic risk factors for localised prostate cancer: a systematic review. Heal Technol Assess Winch Engl 2009;13:iii, xi–xiii 1–219.
41. Magnen CL, Bubendorf L, Rentsch CA, Mengus C, Gsponer JR, Zellweger T, et al. Characterization and clinical relevance of ALDHbright populations in prostate cancer. Clin Cancer Res 2013;19:5361–71.
42. Harada H. How can we overcome tumor hypoxia in radiation therapy? J Radiat Res (Tokyo) 2011;52:545–56.
43. Pistollato F, Rampazzo E, Persano L, Abbadi S, Frasson C, Denaro L, et al. Interaction of hypoxia-inducible factor-1α and Notch signaling regulates medulloblastoma precursor proliferation and fate. Stem Cells 2010;28: 1918–29.
44. Qiang L, Wu T, Zhang HW, Lu N, Hu R, Wang YJ, et al. HIF-1α is critical for hypoxia-mediated maintenance of glioblastoma stem cells by activating Notch signaling pathway. Cell Death Differ 2012;19: 284–94.
45. Duru N, Fan M, Candas D, Menaa C, Liu HC, Nantajit D, et al. HER2-associated radioresistance of breast cancer stem cells isolated from HER2-negative breast cancer cells. Clin Cancer Res 2012;18: 6634–47.
46. Wang Y, Li W, Patel SS, Cong J, Zhang N, Sabbatino F, et al. Blocking the formation of radiation-induced breast cancer stem cells. Oncotarget 2014;5:3743–55.
47. Mao P, Joshi K, Li J, Kim SH, Li P, Santana-Santos L, et al. Mesenchymal glioma stem cells are maintained by activated glycolytic metabolism involving aldehyde dehydrogenase 1A3. Proc Natl Acad Sci U S A 2013; 110:8644–9.
48. Pate KT, Stringari C, Sprowl-Tanio S, Wang K, TeSlaa T, Hoverter NP, et al. Wnt signaling directs a metabolic program of glycolysis and angiogenesis in colon cancer. EMBO J 2014;33:1454–73.
49. Chang L, Graham PH, Hao J, Ni J, Bucci J, Cozzi PJ, et al. Acquisition of epithelial–mesenchymal transition and cancer stem cell phenotypes is associated with activation of the PI3K/Akt/mTOR pathway in prostate cancer radioresistance. Cell Death Dis 2012;4:e875.
50. Chang L, Graham PH, Hao J, Bucci J, Cozzi PJ, Kearsley JH, et al. Emerging roles of radioresistance in prostate cancer metastasis and radiation therapy. Cancer Metastasis Rev 2014;33:469–96.

Cancer Research
The Journal of Cancer Research (1916–1930) | The American Journal of Cancer (1931–1940)

AACR American Association for Cancer Research

Aldehyde Dehydrogenase Is Regulated by β-Catenin/TCF and Promotes Radioresistance in Prostate Cancer Progenitor Cells

Monica Cojoc, Claudia Peitzsch, Ina Kurth, et al.

Cancer Res 2015;75:1482-1494. Published OnlineFirst February 10, 2015.